Surface Waves on a Spherical Earth

1. Upper Mantle Structure from Love Waves

DON L. ANDERSON AND M. NAFI TOKSÖZ

Seismological Laboratory
California Institute of Technology, Pasadena

Abstract. The problem of free oscillations of a heterogeneous sphere is reformulated in terms of dispersion over a plane half-space composed of anisotropic layers having a superposed velocity gradient. This transforms the standing wave discrete spectrum to a traveling-wave continuous spectrum and considerably simplifies the analysis of surface waves on a sphere. Minor modifications make it possible to use any Love wave computer program to compute dispersion on a sphere. Results of the method are compared with those obtained from numerical integration of the exact equations of motion. Agreement is generally better than 0.06 per cent. Dispersion for the fundamental and first seven to eight higher Love modes is presented for a continental and an oceanic path. The oscillatory nature of the group velocity curves becomes more pronounced when a velocity reversal takes place. Calculations of higher-mode group velocity structure and displacement illustrate the mechanism of propagation of the S_a wave. By successive modifications of a previously developed mantle structure, a new suboceanic model is determined which satisfies Love wave and torsional oscillation data.

Introduction. Short-period surface waves are most conveniently treated as traveling waves, and there is a large, well-developed literature concerning surface waves on a flat heterogeneous half-space. The elastic vibrations of the entire earth are best treated as standing waves using normal-mode theory and taking into account, in an exact manner, the effects of sphericity and gravity. Many recent authors have developed and applied this method, but the computations are so formidable that numerical results are available for only a very few earth models. Only the most tentative efforts have been made to modify the standard earth structures to give a more satisfactory fit to the data. The normal-mode approach is especially suited for the low-order oscillations, both conceptually and experimentally. Long-period surface waves may be viewed as a superposition of normal modes, and their dispersion relations follow from the exact free-oscillation solutions.

Alternatively, free oscillations may be regarded as the superposition of traveling waves. This was first pointed out by *Jeans* [1923], but no completely satisfactory method has been presented for computing the dispersion of surface waves traveling around a spherical heterogeneous earth. An 'earth-flattening' approximation has been proposed by *Alterman et al.* [1961] which consists in superposing a linear velocity gradient on the actual structure. Because of the nature of the approximations, the general validity of the method is difficult to assess, but numerical calculations indicate that for simple structures the error reaches 1 per cent for fundamental-mode Rayleigh wave phase velocities at 300 seconds and reaches this error at even shorter periods for Love wave phase velocities. For complicated structures, especially those involving a velocity reversal, the method fails for periods as short as 15 seconds. Calculations for a flat earth are valid only for even shorter periods. In general, the phase velocity curves from flat-earth calculations and the earth flattening approximation bracket the exact spherical solution except at long periods.

Yanovskaya [1958], using asymptotic expansions of the Hankel functions, obtained corrections to the period equation for a layer over a half-space valid for high frequencies.

Bolt and Dorman [1961] and *Kovach and Anderson* [1962] presented approximate empirical formulas relating fundamental-mode dis-

Contribution 1144, Division of Geological Sciences, California Institute of Technology, Pasadena.

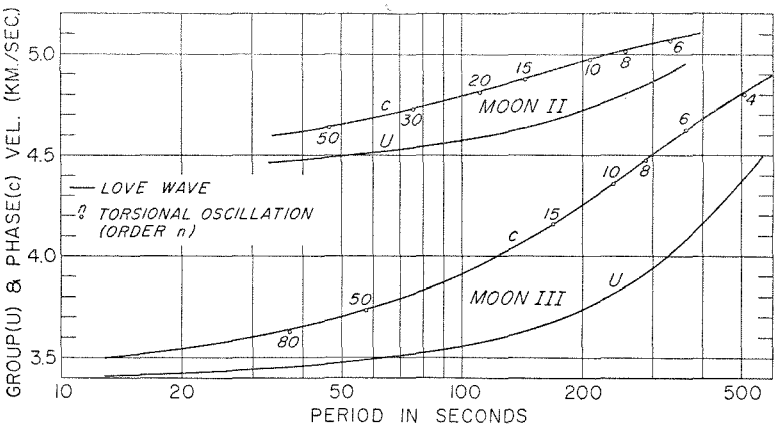

Fig. 1. Love wave dispersion for two moon models compared with exact torsional oscillation results.

persion in a half-space to dispersion in the corresponding sphere. The effect of sphericity on Love waves depends markedly on the structure; it is particularly pronounced for higher modes.

Because of the extreme labor involved in the free-oscillation calculations and the inadequacy of the approximate methods, we develop here a traveling-wave method which is valid over the whole spectrum from short-period crustal waves to the free oscillations. The method is so convenient that dispersion for many models can be quickly determined and the necessary modifications made in order to satisfy the data.

TABLE 1. Dispersion Results for the Fundamental Love Mode, Gutenberg IV Continental Model

Order,* n	T, sec	c, km/sec	U, km/sec
17	411.28	5.5618	4.528
	406.30	5.5500	4.525
18	393.03	5.5054	4.498
	390.27	5.5000	4.497
20	361.30	5.4046	4.449
22	334.55	5.3180	4.414
	328.00	5.300	4.409
24	311.63	5.2431	4.388
32	245.10	5.0253	4.339
	236.42	5.0000	4.330
34	232.74	4.9853	4.333
36	221.59	4.9494	4.329
	220.93	4.9500	4.330
	204.26	4.9000	4.320
40	202.22	4.8878	4.323
	173.31	4.8000	4.319
48	172.16	4.7943	4.318
60	140.79	4.6995	4.315
	140.31	4.7000	4.316
	123.40	4.6500	4.314
70	122.25	4.6448	4.312
76	113.30	4.6186	4.310
	106.33	4.6000	4.309
84	103.23	4.5891	4.306
	89.33	4.5500	4.299
100	87.67	4.5432	4.295

* Free oscillation.

Mathematical formulation. The method is to transform the equations of motion for a homogeneous, isotropic, spherical shell to those for a heterogeneous, anisotropic plane layer with the location of the shell in the layered sequence as a parameter. Haskell matrices are then applied in order to generate an arbitrarily layered sphere. The method is most conveniently introduced for the torsional oscillation or Love wave problem.

Let us consider the radial factor of the steady-state equations of torsional motion for a spherical shell:

$$\mu \frac{d^2v}{dr^2} + \frac{2\mu}{r}\frac{dv}{dr} + \mu\left(\frac{\omega^2}{\beta^2} - \frac{a^2k^2}{r^2}\right)v = 0 \qquad (1)$$

where

μ = rigidity of shell.
a = radius of earth.
β = shear velocity in the shell.
v = transverse displacement.

We have written a^2k^2 instead of the usual separation constant $n(n + 1)$ because we are interested in developing, ab initio, a traveling-wave solution with a continuous spectrum.

TABLE 2. Physical and Computational Parameters for the Gutenberg-Birch Continental Earth Model

N= 36 DELT= 0.C000C10 FK= 0.01000 FKD= 0.00500
NN= 1 DKS= -1.0 CPERT= 1.00100

D	BETA	BETA*	RHO	N	L	XI	DEPTH	M	DPRIME	MUPRIME	RADIUS	X
38.00	3.550	3.561	2.840	35.79110	35.57791	1.006	19.00	1	38.11	35.68434	6351.00	0.9970
12.00	4.600	4.632	3.570	75.54120	74.50122	1.014	44.00	2	12.08	75.01940	6326.00	0.9931
20.00	4.510	4.553	3.507	71.33273	69.99527	1.019	60.00	3	20.19	70.66084	6310.00	0.9906
20.00	4.450	4.5C7	3.486	69.03151	67.30849	1.026	80.00	4	20.25	68.16456	6290.00	0.9874
20.00	4.420	4.490	3.495	68.27972	66.15275	1.032	1C0.00	5	20.32	67.20782	6270.00	0.9843
20.00	4.400	4.484	3.513	68.01168	65.47336	1.039	120.00	6	20.38	66.73045	6250.00	0.9812
20.00	4.390	4.489	3.528	67.99197	65.03615	1.045	140.00	7	20.45	66.49764	6230.00	0.9780
20.00	4.400	4.513	3.546	68.65056	65.24517	1.052	160.00	8	20.52	66.92621	6210.00	0.9749
20.00	4.420	4.549	3.564	69.62773	65.74832	1.059	180.00	9	20.58	67.66022	6190.00	0.9717
20.00	4.450	4.594	3.582	70.93255	66.54831	1.066	200.00	10	20.65	68.70547	6170.00	0.9686
20.00	4.480	4.640	3.606	72.37386	67.46105	1.073	220.00	11	20.72	69.87429	6150.00	0.9655
20.00	4.520	4.697	3.628	74.12149	68.64141	1.080	240.00	12	20.78	71.32884	6130.00	0.9623
20.00	4.570	4.764	3.652	76.27165	70.17246	1.087	260.00	13	20.85	73.15852	6110.00	0.9592
20.00	4.610	4.822	3.676	78.12272	71.40573	1.094	280.00	14	20.92	74.68875	6090.00	0.9560
35.00	4.660	4.896	3.700	80.34772	72.77767	1.104	307.50	15	36.78	76.46908	6062.50	0.9517
50.00	4.810	5.090	3.773	87.29250	77.96345	1.120	350.00	16	52.91	82.49621	6020.00	0.9451
50.00	4.950	5.282	3.848	94.28562	82.81619	1.138	4C0.00	17	53.35	88.36501	5970.00	0.9372
50.00	5.090	5.477	3.924	101.66338	87.80699	1.158	450.00	18	53.80	94.48151	5920.00	0.9294
50.00	5.220	5.665	3.996	108.88460	92.46211	1.178	500.00	19	54.26	100.33793	5870.00	0.9215
50.00	5.360	5.867	4.071	116.95820	97.63326	1.198	550.00	20	54.73	106.85977	5820.00	0.9137
75.00	5.500	6.085	4.147	125.44675	102.48220	1.224	612.50	21	82.98	113.38456	5757.50	0.9038
100.00	5.770	6.482	4.301	143.19276	113.45099	1.262	700.00	22	112.35	127.45729	5670.00	0.8901
100.00	6.040	6.908	4.422	161.32163	123.34573	1.308	800.00	23	114.36	141.06145	5570.00	0.8744
100.00	6.300	7.337	4.543	180.31166	132.95957	1.356	900.00	24	116.45	154.83592	5470.00	0.8587
150.00	6.350	7.568	4.573	184.39478	129.82705	1.420	1025.00	25	178.77	154.72372	5345.00	0.8391
200.00	6.500	8.009	4.694	198.32150	130.63875	1.518	1200.00	26	246.42	160.96109	5170.00	0.8116
200.00	6.600	8.459	4.769	207.73764	126.45881	1.643	1400.00	27	256.34	162.08101	4970.00	0.7802
200.00	6.750	9.014	4.845	220.75031	123.78249	1.783	1600.00	28	267.09	165.30282	4770.00	0.7488
200.00	6.850	9.548	4.920	230.85869	118.82279	1.943	1800.00	29	278.77	165.62390	4570.00	0.7174
200.00	6.950	10.131	4.996	241.31929	113.57325	2.125	2000.00	30	291.53	165.55185	4370.00	0.6860
200.00	7.000	10.693	5.056	247.74400	106.16867	2.333	2200.00	31	305.52	162.18092	4170.00	0.6546
200.00	7.100	11.392	5.116	257.89755	100.17270	2.575	2400.00	32	320.91	160.73050	3970.00	0.6232
200.00	7.200	12.166	5.192	269.15327	94.27651	2.855	2600.00	33	337.93	159.29479	3770.00	0.5918
200.00	7.250	12.936	5.267	276.84668	86.95546	3.184	2800.00	34	356.86	155.15583	3570.00	0.5604
200.00	7.200	13.609	5.267	273.04127	76.42039	3.573	3000.00	35	378.04	144.45041	3370.00	0.5290
20.00	7.200	14.069	5.252	272.26367	71.30928	3.818	3110.00	36	39.08	139.33745	3260.00	0.5118

TABLE 3. Physical and Computational Parameters for the CIT 6 Oceanic Model

N= 36 DELT= 0.0000010 FK= 0.06300 FKD= 0.00500
NW= 1 DKS= 1.0 CPERT= 1.00100

D	BETA	BETA*	RHO	N	L	XI	DEPTH	M	DPRIME	MUPRIME	RADIUS	X
5.00	1.000	1.000	1.000	1.00000	0.99922	1.001	2.50	1	5.00	0.99961	6367.50	0.9996
1.00	1.000	1.001	2.100	2.10000	2.09638	1.002	5.50	2	1.00	2.09819	6364.50	0.9991
5.00	3.700	3.705	2.840	38.87960	38.77591	1.003	8.50	3	5.01	38.82772	6361.50	0.9987
9.00	4.600	4.611	3.535	74.80060	74.43702	1.005	15.50	4	9.02	74.61859	6354.50	0.9976
5.00	4.612	4.628	3.555	75.60039	75.06726	1.007	22.50	5	5.02	75.33335	6347.50	0.9965
5.00	4.612	4.631	3.555	75.60039	74.94905	1.009	27.50	6	5.02	75.27401	6342.50	0.9957
10.00	4.609	4.634	3.550	75.39914	74.57285	1.011	35.00	7	10.06	74.98485	6335.00	0.9945
20.00	4.560	4.596	3.520	73.19989	72.05526	1.016	50.00	8	20.16	72.62532	6320.00	0.9922
20.00	4.450	4.499	3.470	68.69923	67.19765	1.022	70.00	9	20.22	67.94429	6300.00	0.9890
20.00	4.339	4.402	3.420	64.39994	62.59302	1.029	90.00	10	20.29	63.49005	6280.00	0.9859
20.00	4.300	4.376	3.400	62.86600	60.71355	1.035	110.00	11	20.35	61.78040	6260.00	0.9827
20.00	4.290	4.380	3.390	62.39862	59.87773	1.042	130.00	12	20.42	61.12518	6240.00	0.9796
20.00	4.290	4.394	3.390	62.39862	59.49451	1.049	150.00	13	20.48	60.92927	6220.00	0.9765
20.00	4.301	4.419	3.400	62.90109	59.58853	1.056	170.00	14	20.55	61.22241	6200.00	0.9733
20.00	4.322	4.455	3.410	63.70067	59.95730	1.062	190.00	15	20.61	61.80065	6180.00	0.9702
20.00	4.360	4.509	3.462	65.81123	61.54355	1.069	210.00	16	20.68	63.64163	6160.00	0.9670
20.00	4.402	4.566	3.515	68.09990	63.27095	1.076	230.00	17	20.75	65.64103	6140.00	0.9639
20.00	4.460	4.642	3.585	71.29859	65.81198	1.083	250.00	18	20.82	68.50037	6120.00	0.9608
20.00	4.521	4.721	3.625	74.09953	67.95106	1.090	270.00	19	20.89	70.95873	6100.00	0.9576
20.00	4.590	4.809	3.665	77.20113	70.33183	1.098	290.00	20	20.95	73.68647	6080.00	0.9545
20.00	4.660	4.899	3.720	80.79937	73.12642	1.105	310.00	21	21.02	76.86721	6060.00	0.9513
20.00	4.741	5.000	3.760	84.49956	75.97128	1.112	330.00	22	21.09	80.12203	6040.00	0.9482
20.00	4.824	5.105	3.790	88.20065	78.77455	1.120	350.00	23	21.16	83.35446	6020.00	0.9451
40.00	4.911	5.223	3.830	92.37540	81.68289	1.131	380.00	24	42.54	86.86478	5990.00	0.9403
50.00	5.040	5.400	3.890	98.80046	86.05653	1.148	425.00	25	53.57	92.20859	5945.00	0.9333
50.00	5.210	5.630	3.950	107.21919	91.82507	1.168	475.00	26	54.03	99.22404	5895.00	0.9254
100.00	5.450	5.965	4.010	119.09828	99.41973	1.198	550.00	27	109.45	108.81507	5820.00	0.9137
100.00	5.760	6.415	4.210	139.70194	112.64596	1.240	650.00	28	111.36	125.44664	5720.00	0.8980
100.00	6.030	6.835	4.400	159.99857	124.54028	1.285	750.00	29	113.35	141.16043	5620.00	0.8823
100.00	6.230	7.190	4.560	176.99818	132.91319	1.332	850.00	30	115.40	153.37990	5520.00	0.8666
100.00	6.322	7.430	4.630	185.04452	133.96641	1.381	950.00	31	117.53	157.44761	5420.00	0.8509
200.00	6.421	7.761	4.740	195.40225	133.74327	1.461	1100.00	32	241.75	161.65932	5270.00	0.8273
200.00	6.550	8.230	4.850	208.10253	131.83005	1.579	1300.00	33	251.28	165.63263	5070.00	0.7959
200.00	6.690	8.751	4.960	221.99689	129.75555	1.711	1500.00	34	261.60	169.72132	4870.00	0.7645
200.00	6.780	9.248	5.070	233.05978	125.26283	1.861	1700.00	35	272.81	170.86172	4670.00	0.7331
-0.	7.150	9.966	5.490	280.66251	144.45678	1.943	1800.00	36	-0.	201.35443	4570.00	0.7174

TABLE 4. Physical and Computational Parameters for the CIT 11 Oceanic Earth Model

N= 46 DELT= 0.0000010 FK= 0.01000 FKD= 0.00500
NW= 1 DKS= 1.0 CPERT= 1.00100

D	BETA	BETA*	RHO	N	L	XI	DEPTH	M	DPRIME	MUPRIME	RADIUS	X
5.00	1.000	1.000	1.000	1.00000	0.99922	1.001	2.50	1	5.00	0.99951	6367.50	0.9996
1.00	1.000	1.001	2.100	2.10000	2.09638	1.002	5.50	2	1.00	2.09819	6364.50	0.9991
5.00	3.700	3.705	2.840	38.87960	38.77591	1.003	8.50	3	5.01	38.82772	6361.50	0.9987
9.00	4.600	4.611	3.535	74.80060	74.43702	1.005	15.50	4	9.02	74.61859	6354.50	0.9976
5.00	4.612	4.628	3.555	75.60039	75.06726	1.007	22.50	5	5.02	75.33335	6347.50	0.9965
5.00	4.612	4.631	3.555	75.60039	74.94905	1.009	27.50	6	5.02	75.27401	6342.50	0.9957
10.00	4.609	4.634	3.550	75.39914	74.57285	1.011	35.00	7	10.06	74.98485	6335.00	0.9945
20.00	4.560	4.596	3.520	73.19989	72.05526	1.016	50.00	8	20.16	72.62532	6320.00	0.9922
20.00	4.449	4.499	3.470	68.69923	67.19765	1.022	70.00	9	20.22	67.94429	6300.00	0.9890
20.00	4.339	4.402	3.420	64.39994	62.59302	1.029	90.00	10	20.29	63.49005	6280.00	0.9859
20.00	4.340	4.416	3.400	64.04104	61.84836	1.035	110.00	11	20.35	62.93515	6260.00	0.9827
20.00	4.340	4.430	3.390	63.85268	61.27304	1.042	130.00	12	20.42	62.54957	6240.00	0.9796
20.00	4.340	4.445	3.390	63.85268	60.88090	1.049	150.00	13	20.48	62.34909	6220.00	0.9765
20.00	4.500	4.623	3.400	68.85000	65.22415	1.056	170.00	14	20.55	67.01256	6200.00	0.9733
20.00	4.500	4.638	3.410	69.05250	64.99463	1.062	190.00	15	20.61	66.99285	6180.00	0.9702
20.00	4.500	4.653	3.462	70.10550	65.55935	1.069	210.00	16	20.68	67.79433	6160.00	0.9670
20.00	4.500	4.669	3.515	71.17875	66.13148	1.076	230.00	17	20.75	68.60872	6140.00	0.9639
20.00	4.500	4.684	3.585	72.59625	67.00977	1.083	250.00	18	20.82	69.74710	6120.00	0.9608
20.00	4.500	4.699	3.625	73.40625	67.31531	1.090	270.00	19	20.89	70.29484	6100.00	0.9576
20.00	4.500	4.715	3.665	74.21625	67.61255	1.098	290.00	20	20.95	70.83749	6080.00	0.9545
20.00	4.500	4.730	3.720	75.33000	68.17644	1.105	310.00	21	21.02	71.66402	6060.00	0.9513
20.00	4.500	4.746	3.760	76.14000	68.45543	1.112	330.00	22	21.09	72.19554	6040.00	0.9482
20.00	4.500	4.762	3.790	76.74750	68.54540	1.120	350.00	23	21.16	72.53060	6020.00	0.9451
40.00	4.800	5.105	3.830	88.24320	78.02900	1.131	380.00	24	42.54	82.97908	5990.00	0.9403
50.00	5.040	5.400	3.890	98.80046	86.05653	1.148	425.00	25	53.57	92.20859	5945.00	0.9333
10.00	5.400	5.815	3.950	115.18200	99.31509	1.160	455.00	26	10.77	106.95471	5915.00	0.9286
140.00	5.400	5.890	4.010	116.93160	98.28307	1.190	530.00	27	152.71	107.20259	5840.00	0.9168
100.00	5.400	6.014	4.210	122.76359	98.98805	1.240	650.00	28	111.36	110.23670	5720.00	0.8980
100.00	6.200	7.027	4.400	169.13600	131.65271	1.285	750.00	29	113.35	149.22202	5620.00	0.8823
100.00	6.230	7.189	4.560	176.98681	132.90466	1.332	850.00	30	115.40	153.37005	5520.00	0.8666
100.00	6.322	7.430	4.630	185.04452	133.96641	1.381	950.00	31	117.53	157.44761	5420.00	0.8509
200.00	6.421	7.761	4.740	195.40225	133.74327	1.461	1100.00	32	241.75	161.65932	5270.00	0.8273
200.00	6.550	8.230	4.850	208.10253	131.83005	1.579	1300.00	33	251.28	165.63263	5070.00	0.7959
200.00	6.690	8.751	4.960	221.99689	129.75555	1.711	1500.00	34	261.60	169.72132	4870.00	0.7645
200.00	6.780	9.248	5.070	233.05978	125.26283	1.861	1700.00	35	272.81	170.86172	4670.00	0.7331
150.00	6.850	9.707	5.150	241.65087	120.32861	2.008	1875.00	36	212.57	170.52129	4495.00	0.7057
100.00	6.900	10.058	5.208	247.95287	116.69524	2.125	2000.00	37	145.77	170.10257	4370.00	0.6860
100.00	6.950	10.368	5.270	254.55417	114.38184	2.225	2100.00	38	149.18	170.63521	4270.00	0.6703
100.00	7.000	10.693	5.320	260.67999	111.71229	2.333	2200.00	39	152.76	170.64923	4170.00	0.6546
100.00	7.050	11.034	5.370	266.93241	108.95884	2.450	2300.00	40	156.51	170.53262	4070.00	0.6389
100.00	7.100	11.392	5.420	273.22219	106.12510	2.575	2400.00	41	160.45	170.28133	3970.00	0.6232
100.00	7.140	11.752	5.470	278.85840	102.92640	2.709	2500.00	42	164.60	169.41633	3870.00	0.6075
100.00	7.190	12.149	5.520	285.36246	99.95412	2.855	2600.00	43	168.97	168.88799	3770.00	0.5918
100.00	7.230	12.549	5.560	290.63731	96.47274	3.013	2700.00	44	173.57	167.44724	3670.00	0.5761
100.00	7.280	12.990	5.610	297.32101	93.38630	3.184	2800.00	45	178.43	166.63045	3570.00	0.5604
100.00	7.300	13.401	5.660	301.62138	89.50395	3.370	2900.00	46	183.57	164.30552	3470.00	0.5447

With the substitution $r = a - h$, where h is the depth variable, we obtain

$$\mu \frac{d^2v}{dh^2} - \frac{2\mu}{(a-h)} \frac{dv}{dh} + \mu\left(\frac{\omega^2}{\beta^2} - \frac{a^2k^2}{(a-h)^2}\right)v = 0 \qquad (2)$$

and we define the new variable

$$\chi(h) = (a - h)v(h)$$

Equation 2 then becomes

$$\mu \frac{d^2\chi}{dh^2} + \mu\left(\frac{\omega^2}{\beta^2} - \frac{a^2k^2}{(a-h)^2}\right)\chi = 0 \qquad (3)$$

This resembles the equation of motion for a plane layer except for the factor $a^2/(a - h)^2$ which arises from the curvature of the earth.

We can rewrite (3) as

$$\mu\left(\frac{a-h}{a}\right)^2 \frac{d^2\chi}{dh^2} + \mu\left[\frac{\omega^2}{\beta^2\left(\frac{a}{a-h}\right)^2} - k^2\right]\chi = 0 \qquad (4)$$

The expression in brackets is the same as the corresponding flat-earth expression except that the velocity is modified by the linear factor $a/(a - h)$. This effective linear increase in velocity is due to sphericity. It was taken into account by Alterman, Jarosch, and Pekeris in their earth-flattening approximation. The effect on the first term in (4) did not appear in their formulation. This additional factor effectively introduces an anisotropy which increases with depth.

Equation 4 is the equation of motion for a spherical shell and is exact. For a sufficiently thin shell bounded by h_i and h_{i+1}, or r_i and r_{i+1}, we take

$$\left(\frac{a-h}{a}\right)^2 = \left(\frac{r_m}{a}\right)^2 = \xi$$

where $r_{i+1} < r_m < r_i$. With this, (4) becomes

$$\mu\xi \frac{d^2\chi}{dh^2} + \mu\left[\frac{\omega^2\xi}{\beta^2} - k^2\right]\chi = 0 \qquad (5)$$

In the mth layer we can rewrite (5) as

$$L_m \frac{d^2\chi_m}{dh^2} + N_m\left[\frac{\omega^2}{\beta_{2_m}^2} - k^2\right]\chi_m = 0 \qquad (6)$$

which is in the form of the displacement equation of motion for a transversely isotropic plane layer with a modified velocity. In the context of anisotropic theory [*Anderson*, 1962], ξ^{-1} is the anisotropy factor. The mapping of a sphere into a plane half-space therefore superposes a linear velocity gradient and a linearly increasing ani-

TABLE 5. Fundamental Love Mode Results for the Gutenberg-Birch Model

Order,* n	T, sec	c, km/sec	U, km/sec
	664.53	6.200	5.089
	442.06	5.650	4.603
	408.32	5.550	4.541
	393.737	5.50615	4.5164
18	392.977	5.50615	4.513
	375.74	5.450	4.487
	361.731	5.40665	4.4655
20	361.165	5.40665	4.463
	344.02	5.350	4.440
	312.94	5.250	4.400
24	311.41	5.247	4.397
	297.56	5.200	4.382
26	291.52	5.182	4.374
	282.27	5.150	4.366
	258.839	5.07354	4.3443
30	258.688	5.07354	4.343
	251.83	5.050	4.338
32	244.96	5.028	4.331
	236.64	5.000	4.325
34	232.641	4.98748	4.321
	232.713	4.98748	4.3227
	221.565	4.95073	4.3142
36	221.526	4.95073	4.313
	221.47	4.950	4.314
42	193.84	4.859	4.293
	191.13	4.850	4.292
50	166.252	4.76791	4.2735
	166.145	4.76791	4.2751
	160.85	4.750	4.271
52	160.56	4.749	4.269
	130.92	4.650	4.245
66	129.59	4.645	4.242
90	97.60	4.532	4.195
	96.77	4.530	4.19
100	88.56	4.498	4.173
	83.89	4.480	4.16
	72.39	4.430	4.11
	48.32	4.28	3.89
	43.25	4.230	3.80
	35.60	4.13	3.65
	20.13	3.83	3.44
	15.23	3.73	3.45

* Free oscillation.

TABLE 6. Second Love Mode Results for the Gutenberg-Birch Model

Order,* n	T, sec	c, km/sec	U, km/sec
	207.55	7.650	5.450
	194.31	7.450	5.321
	181.48	7.250	5.191
	175.22	7.150	5.127
	162.98	6.950	5.00
	145.19	6.650	4.841
	139.37	6.550	4.793
	122.07	6.250	4.664
	110.59	6.050	4.589
	99.09	5.85	4.520
	98.21	5.800	4.503
72	95.44	5.785	
80	87.94	5.655	
	87.56	5.650	4.453
	84.67	5.600	4.437
84	84.64	5.597	
	78.91	5.500	4.405
	73.14	5.400	4.373
	67.37	5.300	4.344
	61.59	5.200	4.317
	55.8	5.100	4.296
	49.88	5.000	4.282
	43.83	4.900	4.282
	37.40	4.800	4.301
	30.17	4.700	4.347
	21.02	4.600	4.414
	9.495	4.300	3.354
	7.198	4.00	3.280

* Free oscillation.

sotropy on the original structure. It can be called the *earth-stretching approximation* because of the distortion introduced.

The solution of (6) is

$$\chi_m(h) = \chi_{1m} \sin k\zeta_m h + \chi_{2m} \cos k\zeta_m h \qquad (7)$$

$$h_m < h < h_{m+1}$$

where

$$\zeta_m = \xi^{-1/2}\left(\frac{c^2}{\beta_{2m}{}^2} - 1\right)^{1/2} \qquad (8)$$

We can now follow the procedure of *Anderson* [1962] and introduce pseudo-parameters to transform the plane anisotropic layer to a plane isotropic layer and proceed directly to a solution.

Since we know the solution for a single shell, the generalization to a concentrically layered sphere is a straightforward application of Haskell's method [*Haskell*, 1951; *Anderson*, 1962]. The matrix manipulations are facilitated by the use of addition theorems which can be invoked because of the trigometric form of (7). This form also considerably simplifies the calculation of such quantities as energy and group velocity.

Numerical computation. A Fortran program written to compute Love wave dispersion on a flat-layered, isotropic half-space by D. Harkrider (1962, unpublished) was modified according to the above theory and used in computing dispersion on a layered sphere for a variety of earth and moon modes, including higher modes. If no initial knowledge of the dispersion is available, it takes approximately 3 minutes to calculate and verify 30 points on a dispersion curve with an IBM 7090 computer. The accuracy of the calculations at various stages of solution is checked automatically by the following tests:

TABLE 7. Fundamental Love Mode Results for CIT 6 Oceanic Model

Order,* n	T, sec	c, km/sec	U, km/sec
14	475.62	5.804	
	470.86	5.800	4.686
	411.62	5.620	4.56
	408.44	5.610	4.56
	405.27	5.600	4.557
18	380.38	5.542	
	364.91	5.470	4.49
	349.72	5.420	4.46
	334.66	5.370	4.44
22	332.39	5.352	
	313.75	5.300	4.4208
	260.30	5.120	4.37
30	257.37	5.099	
	254.34	5.100	4.369
	224.30	5.000	4.355
	215.18	4.970	4.35
40	201.16	4.913	
	199.82	4.92	4.34
	168.31	4.820	4.34
	161.85	4.800	4.348
	154.65	4.760	4.399
54	154.13	4.765	
	146.79	4.740	4.391
	135.28	4.720	4.35
	128.42	4.700	4.356
	99.79	4.620	4.36
94	92.31	4.588	
	92.26	4.600	4.370
	72.50	4.550	4.37
	61.68	4.500	4.380
	28.30	4.400	3.948
	25.61	4.300	2.984

* Free oscillation.

TABLE 8. Second Love Mode Results for CIT 6 Oceanic Model

Order,* n	T, sec	c, km/sec	U, km/sec
72	95.18	5.800	
	94.39	5.800	4.490
74	93.20	5.765	
	88.79	5.700	4.461
	83.17	5.600	4.434
92	78.58	5.507	
	77.50	5.500	4.407
	71.80	5.400	4.381
	66.06	5.300	4.357
	60.29	5.200	4.333
	54.47	5.100	4.311
	48.61	5.000	4.291
	42.71	4.900	4.269
	36.85	4.800	4.238
	31.30	4.700	4.166
	28.84	4.650	4.097
	26.70	4.600	4.024
	24.66	4.550	4.046
	22.98	4.517	4.172
	14.47	4.450	4.379
	9.261	4.350	3.378
	8.71	4.25	2.844
	8.26	4.100	2.124

* Free oscillation.

1. Total kinetic energy equals total potential energy.
2. Determinant of the Haskell product matrix is unity.
3. Displacement converges with depth.
4. Energy velocity equals group velocity.

An additional check is obtained by comparing the results with solutions obtained from numerical integration of the exact equations of motion when this information is available. Usually, the results for this 'pseudo-spherical' or 'earth-stretching' method and the 'exact' spherical method agreed to better than 0.06 per cent when the equations of motion were numerically integrated with high precision. It should be noted here that the so-called 'exact' solutions are usually obtained by numerical integration of the exact equations of motion and are subject to round-off, starting-point, and step-size errors. On the other hand, the approximate method presented here is evaluated exactly and is not subject to such errors. In any event the accuracy of the new method is at least an order of magnitude higher than the experimental uncertainty,

TABLE 9. Third Love Mode Results for CIT 6 Oceanic Model

T, sec	c, km/sec	U, km/sec
46.35	5.620	4.40
44.86	5.570	4.39
40.35	5.42	4.34
35.87	5.27	4.28
30.02	5.07	4.19
26.72	4.950	4.108
25.18	4.890	4.047
23.74	4.830	3.995
21.29	4.730	4.062
17.75	4.630	4.275
14.59	4.570	4.328
10.62	4.470	3.995
6.10	4.390	2.967
5.73	4.250	2.698

and it can be improved by simply reducing layer thicknesses.

Energy and group velocities are calculated exactly by the integration of energy integrals and analytical differentiation of the product matrix form of the period equation [*Harkrider and Anderson,* 1963]. Group velocities are also calculated by numerical differentiation as a check on this widely used procedure. If this option is left out, the above-quoted computation time is reduced by a third. Analytical partial derivatives [*Anderson,* 1963] are also calculated routinely for each parameter and these calculations are included in the above time estimate. These partial derivatives are used to modify test structures when a fit to data is being attempted.

As a first test of the method, dispersion was computed for two moon models. The effect of sphericity on such a small body appears at very short periods, so this is a severe test. Also the

TABLE 10. Fourth Love Mode Results for CIT 6 Oceanic Model

T, sec	c, km/sec	U, km/sec
21.38	5.00	3.817
20.51	4.940	3.896
18.70	4.840	4.092
16.26	4.740	4.211
13.35	4.640	4.234
10.05	4.540	4.321
7.934	4.500	4.371

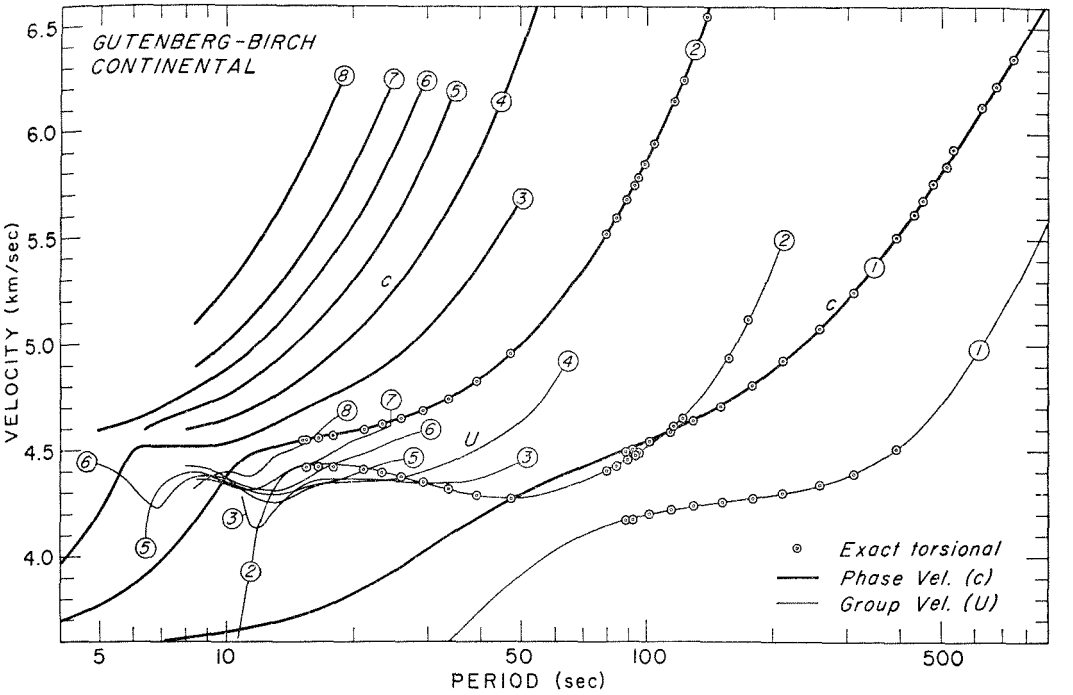

Fig. 2. Dispersion for the first eight Love modes on a spherical earth having a Gutenberg-Birch continental structure. Exact torsional results for periods greater than 400 seconds are for the Gutenberg IV model calculated by *MacDonald and Ness* [1961].

periods of torsional oscillations have been worked out by *Carr and Kovach* [1962]. Figure 1 gives the *earth-stretching* results (solid line) and the 'exact' torsional oscillation results (circles) of Carr and Kovach.

Models. Dispersion has been computed using the above method for a variety of continental and oceanic earth models; ten higher modes have been computed for some models. Detailed results will be presented here for one continental (Gutenberg-Birch) and one oceanic (CIT 6) structure. These structures are described by *Kovach and Anderson* [1962]. Partial results for other models which were successive approximations to a satisfactory earth structure are presented in a later section. Fragmentary results for a Jeffreys-Bullen model are also shown for comparison. We know from previous work [*Dorman et al.*, 1960; *Kovach and Anderson*, 1962] that this structure does not satisfy surface wave data. Results for a modification of a model designated Gutenberg IV by *MacDonald and Ness* [1961] are listed in Table 1 for comparison with the free-oscillation calculations which were calculated by Kovach (personal communication) using an improved version of the program described by *Kovach and Anderson* [1962].

The parameters of the models under present consideration are given in Tables 2, 3, and 4. To avoid transcribing errors each table is a photograph of the first page of output from the computer for a given computation. The first two lines of data are computational parameters and are not relevant to the present discussion. The notation for the column headings is:

D	Layer thickness
BETA	Shear velocity in layer
BETA*	Transformed shear velocity (β_2)
RHO	Density
N, L	Directional rigidities
XI	Anisotropy factor
DEPTH	Depth to layer midpoint
M	Layer number
DPRIME	Pseudo-thickness [*Anderson*, 1962]
MUPRIME	Pseudo-rigidity [*Anderson*, 1962]
RADIUS	Radius from center of earth to layer midpoint (R)
X	R/a where a = earth radius

The column marked XI illustrates the increasing anisotropy with depth that results when

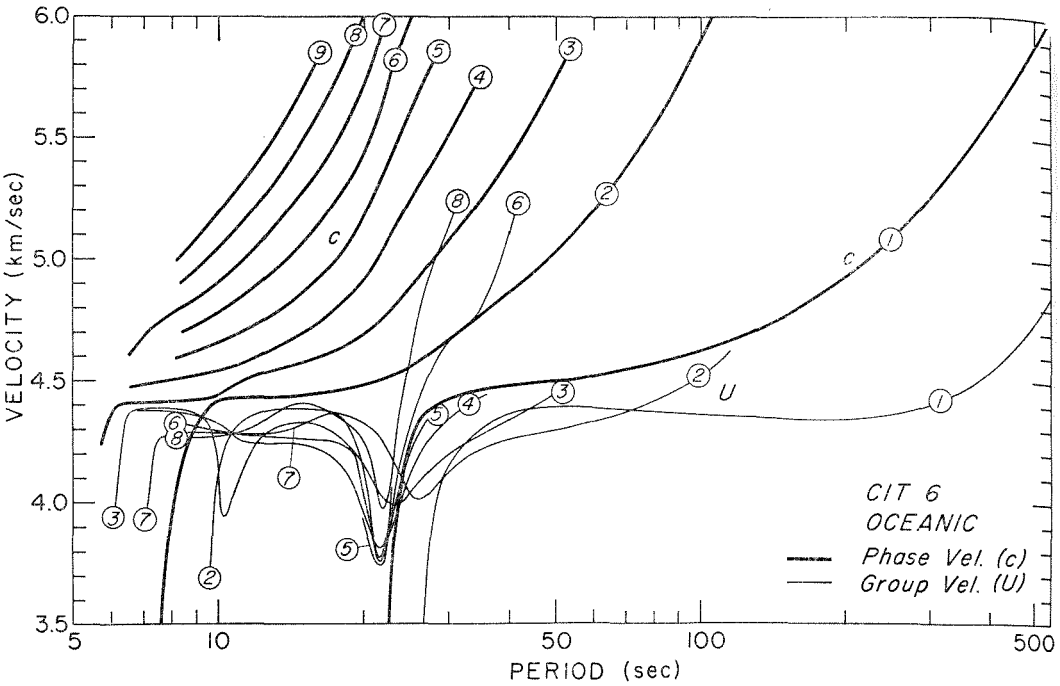

Fig. 3. Dispersion for the first nine Love modes on a spherical earth with a CIT 6 oceanic structure.

a layered sphere is mapped onto a layered half-space.

The results for these models are given in Tables 5 through 10 and Figures 2, 3, and 4. For comparison, some results of the numerical integration of the exact equations of motion are also given.

Phase (c) and group (U) velocities are shown for the first eight Love modes in Figure 2 for the Gutenberg-Birch structure. This model has a slight reversal in the upper mantle for both shear velocity and density. The minimums in the group velocities between 10 and 15 seconds are associated with this channel. The oscillatory

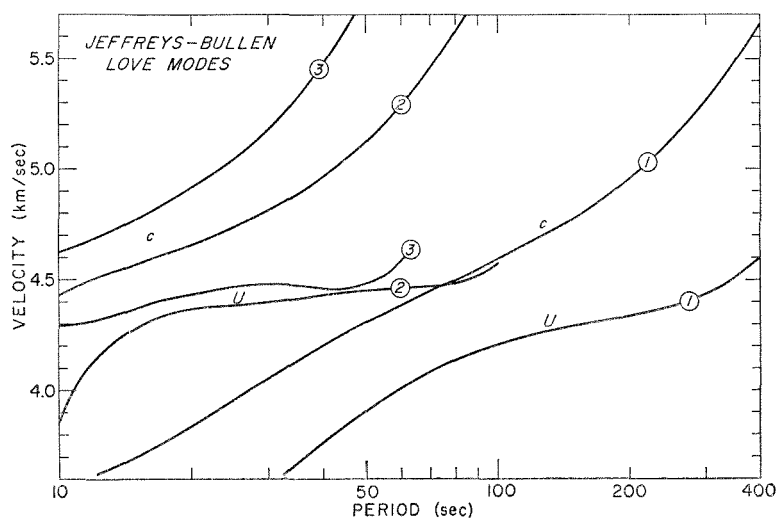

Fig. 4. Dispersion for the first three Love modes on a spherical earth with a Jeffreys-Bullen structure.

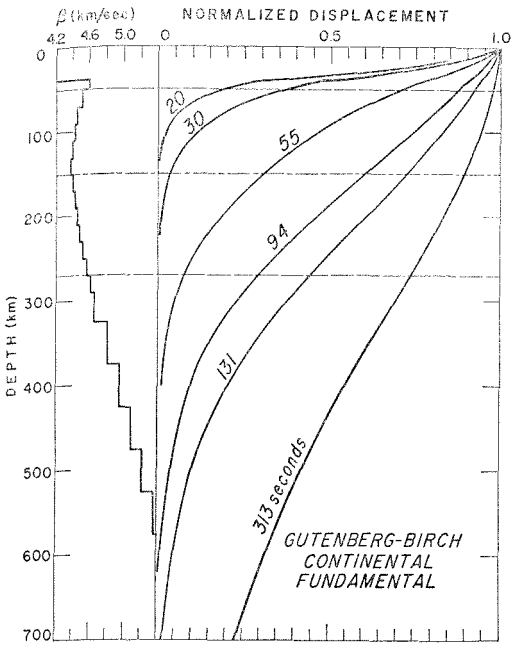

Fig. 5. Displacements versus depth for the fundamental Love mode, Gutenberg-Birch continental structure.

nature of the higher-mode group velocities is a basic property even for the simplest structures, but it is accentuated and distorted when a channel is present. Contrast these results, for example, with the Jeffreys-Bullen model in Figure 4. Also shown in Figure 2 and Table 5 are results from the exact torsional oscillation program described by *Kovach and Anderson* [1962]. The agreement is considered excellent, especially since the methods approximate the structure in slightly different ways.

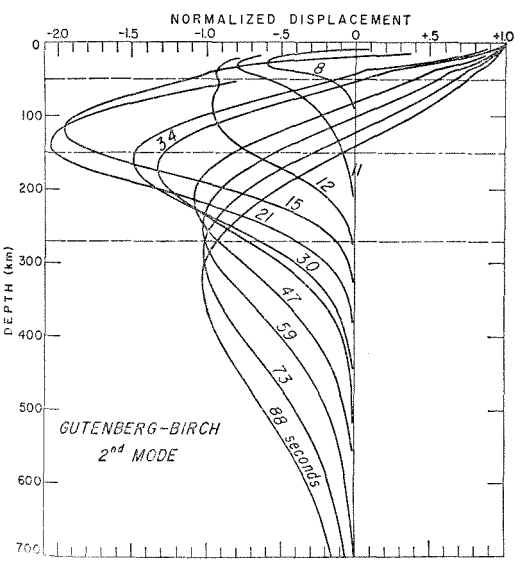

Fig. 6. Displacements versus depth for the second Love mode, Gutenberg-Birch continental structure.

The maximums and minimums of the group velocity curves are of particular interest because they produce relatively large amplitude arrivals. The fundamental has no extremum beyond 30 seconds but only a broad inflection between 100 and 300 seconds. A long-period continental Love wave will therefore tend to be oscillatory. The first higher mode (second Love mode) has a broad minimum centered at about 46 seconds with a group velocity of 4.28 km/sec and a broad maximum at 17 seconds with a group velocity of 4.43 km/sec. This maximum is appropriate in both velocity and period for the continental S_a wave. The continental S_a wave with period 14 to 20 seconds is unquestionably associated with the long-period maximum of the first higher Love mode. It is possible that the arrival controlled by this maximum may sometimes be picked as the beginning of the so-called continental G or LQ wave.

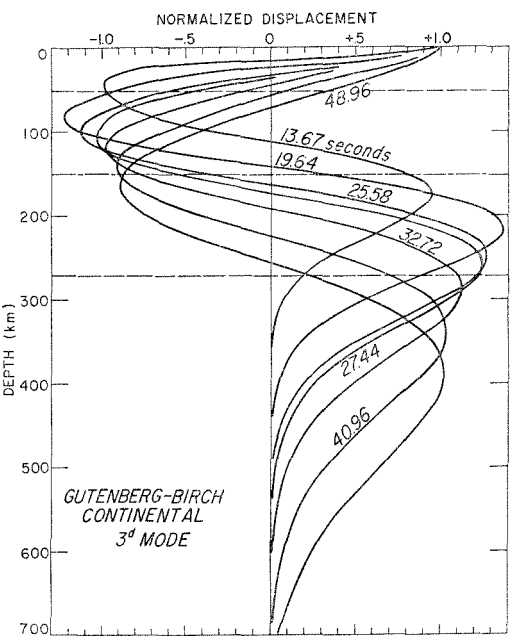

Fig. 7. Displacements versus depth for the third Love mode, Gutenberg-Birch continental structure.

The third Love mode has a broad plateau between 15 and 40 seconds with a group velocity of about 4.35 km/sec, and a sharp minimum at about 12 seconds with a velocity of about 4.13 km/sec. The other higher modes tend to have maximums around 8 to 10 seconds at 4.4 km/sec. Some of *Caloi*'s [1954] reported S_a waves have this property. The shorter-period continental S_a waves are therefore probably associated with higher-mode group velocity maximums. This agreement leads us to propose that S_a waves be defined as higher mantle Love modes with completely transverse horizontal motion. The vertical component sometimes reported is probably associated with Rayleigh motion, and a different designation is desirable.

Further information about the mechanism of propagation at those waves can be obtained from plots of displacement versus depth. The fundamental-mode displacement (Figure 5) decays monotonically with depth with a slight inflection at the crust-mantle boundary. The presence of the low-velocity zone keeps the displacements greater in the upper mantle than they would otherwise be. Three horizontal lines drawn on the displacement graphs represent the top, center, and bottom of the low-velocity zone. The second Love mode (Figure 6) clearly illustrates the wave-guide nature of the low-velocity zone. Between 15 and 30 seconds the negative lobe of the displacement is in the top half of the low-velocity zone and is much greater than the corresponding lobe for shorter or longer periods. In this range of periods the phase velocity is approximately the same as the shear velocity of the 'lid' of the low-velocity zone. These periods are therefore effectively 'trapped' in the low-velocity zone and a true channel wave results. When the phase velocity becomes less than the minimum channel velocity, the wave becomes untrapped and the displacements again take on their familiar, simple exponential behavior. These displacements indicate that a source between 50 and 200 km will be especially effective in generating the 15- to 30-second S_a wave. This also agrees with Caloi's observations concerning this wave. The other higher modes (Figures 7 and 8) exhibit a corresponding behavior.

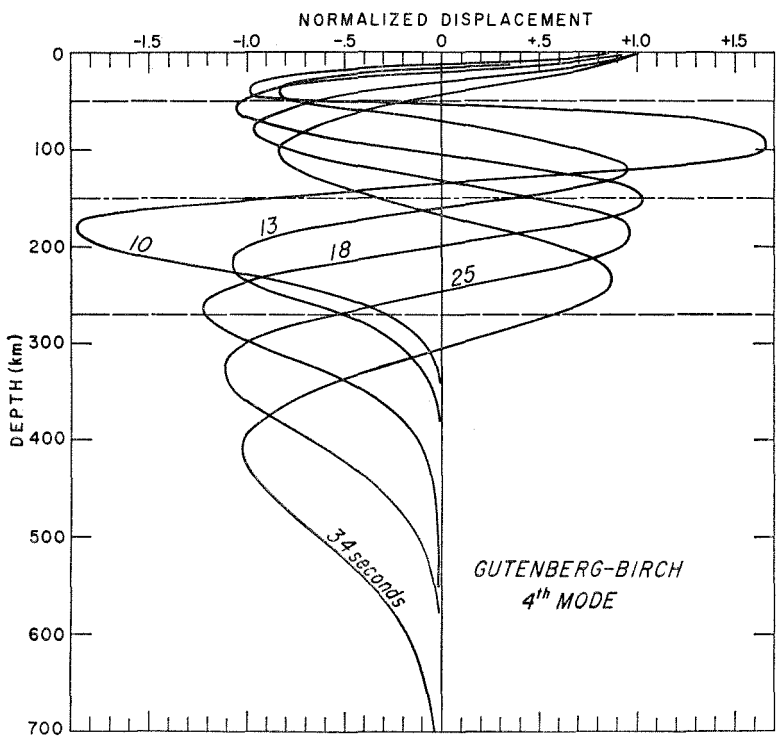

Fig. 8. Displacements versus depth for the fourth Love mode, Gutenberg-Birch continental structure.

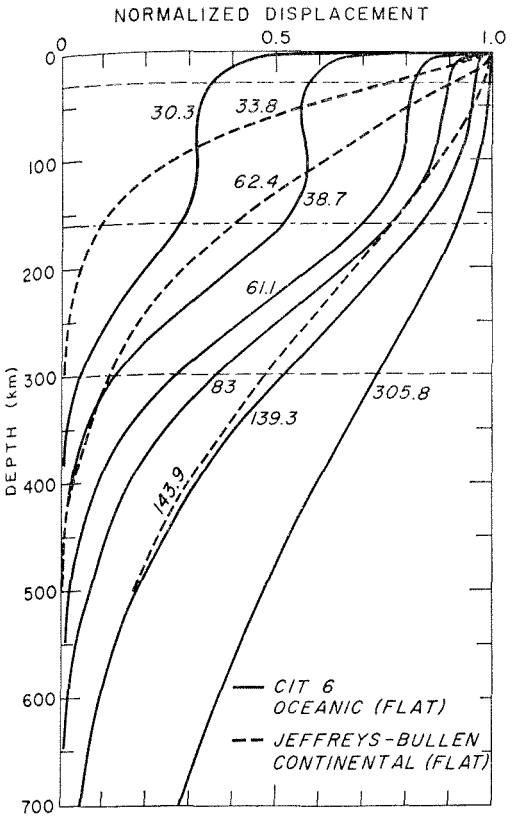

Fig. 9. Comparison between displacements versus depth for the Jeffreys-Bullen (no low-velocity zone) and CIT 6 (low-velocity zone) models based on calculations for a flat earth.

CIT 6 is an oceanic model that has been shown to give good agreement with data for oceanic Love wave phase velocities [*Kovach and Anderson*, 1962]. It is characterized by a shallow and extreme low-velocity, low-density layer in the upper mantle. Group velocity minimums are very pronounced in this model, and many of the modes show a strong narrow minimum at about 22 seconds and about 3.75 km/sec. This behavior is again associated with the low-velocity zone, as illustrated by the displacement graphs. A broad maximum between 10 and 20 seconds with group velocity between 4.25 and 4.4 km/sec occurs for each mode. Between 50 and 200 seconds the fundamental-mode group velocity curve is contained between 4.3 and 4.4 km/sec, and this is responsible for the well-known pulse nature of the G wave. The second- and third-mode group velocities both cross the fundamental group velocity between 29 and 70 seconds. The resulting interference makes mode separation difficult in this region. The second mode has a sharp minimum at 26 seconds with group velocity of 4 km/sec. Combining information from all the modes, we find for the oceanic S_a wave a 7- to 9-second wave arriving with a velocity of 4.4 km/sec riding on a 12- to 20-second wave with the same initial arrival time. Both groups will be oscillatory because of the adjacent pronounced group velocity troughs. This closely duplicates the behavior of some of Caloi's published records.

Caloi explained the S_a waves as waves propagated in a low-velocity asthenosphere channel. *Oliver and Ewing* [1958] speculated that the properties of the S_a phase would emerge from a complete normal-mode analysis of a realistic earth model when the effects of curvature and velocity gradients were taken into account. They state that the 'identification of S_a with a deep channel in the mantle is suspect until the other

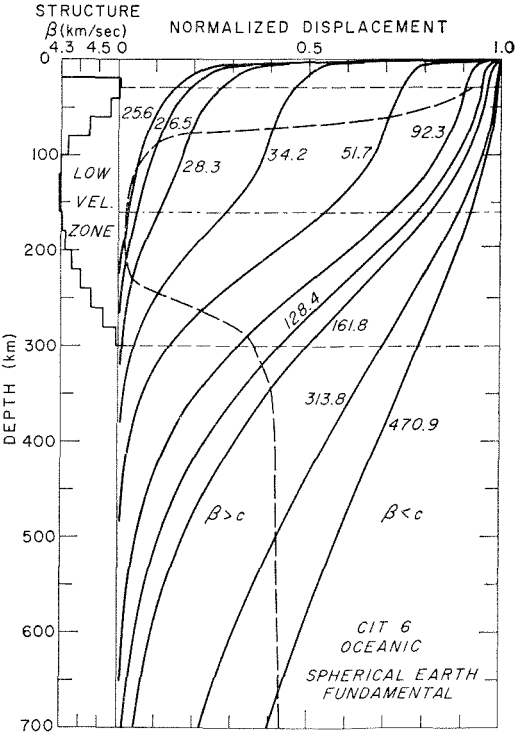

Fig. 10. Displacement versus depth for the CIT 6 oceanic fundamental mode. The dashed line separates the regions for β greater than or less than c and indicates the effective width of the low-velocity zone for each period.

possible mechanisms are eliminated.' The present analysis indicates that there are elements of truth in both of the above viewpoints. A low-velocity zone seems to be necessary to explain the sharp beginning, the large amplitudes, and the oscillatory nature of the S_a wave as well as the comments about its excitation as a function of focal depth. When a low-velocity layer is present in the upper mantle the displacement-depth graphs show that a true channel wave does result from a normal-mode analysis as performed in this paper.

The displacements for this model, which has a particularly pronounced low-velocity zone, are compared with displacements in the Jeffreys-Bullen model having no low-velocity zone in Figure 9. This clearly illustrates how effectively the displacements are trapped by the channel. Figures 10, 11, and 12 are graphs of displacement versus depth for the first four Love modes. The exaggeration of the displacement lobes that are caught in the low-velocity channel are even more pronounced than for the continental model.

Oceanic mantle structure. Dispersion data, primarily phase velocities, from a variety of sources, including free oscillations, are given in Figure 13. Most of the data are for complete great-circle paths. The great-circle path which includes New Guinea and Pasadena is the most oceanic (90 per cent) and probably the most reliable of the data below 300 seconds. Several points for the Mongolia-Pasadena path (65 per cent oceanic) were corrected approximately to a completely oceanic path before a theoretical fit was attempted. *Toksöz and Ben-Menahem* [1963] give details of these phase velocity determinations.

These data and the free-oscillation data of *Smith* [1961] show the least scatter and form the primary basis of the following analysis. The scatter of the remaining data is due partially to experimental technique and partially to path

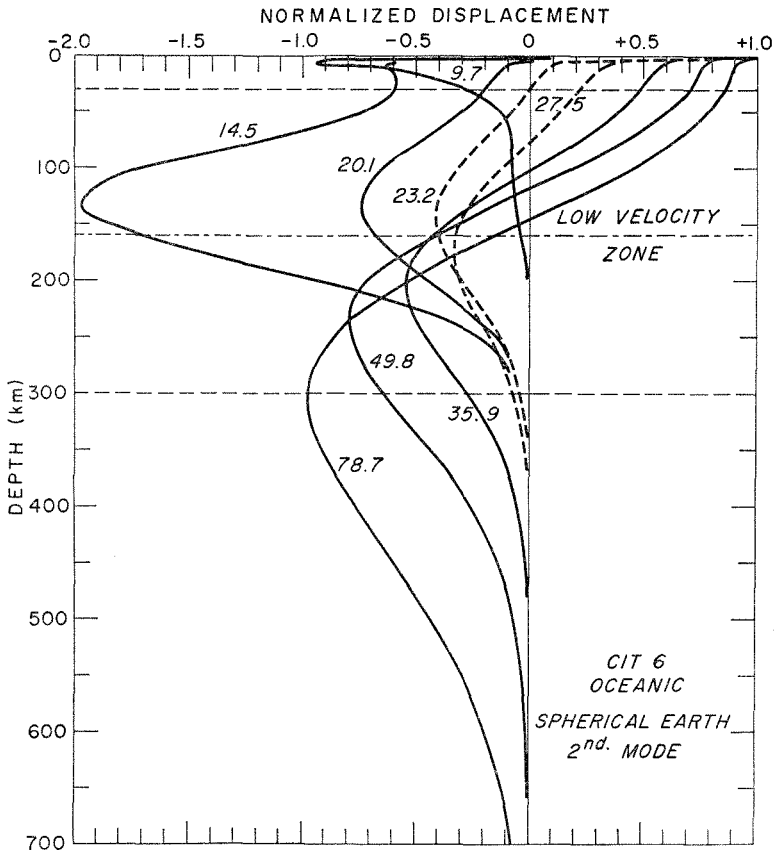

Fig. 11. Displacements versus depth for the second Love mode, CIT 6 structure.

TABLE 11. Results for Successive Approximations to an Oceanic Structure

	CIT 8		CIT 9		CIT 10		CIT 11	
c, km/sec	T, sec	U, km/sec	T, km/sec	U, km/sec	T, sec	U, km/sec	T, sec	U, km/sec
6.25					662.58	5.128	663.86	5.133
6.0					553.59	4.865	554.11	4.871
5.8					477.63	4.681	479.12	4.705
5.7					443.79	4.619	444.44	4.636
5.6					411.00	4.565	411.09	4.576
5.5					379.00	4.517	378.75	4.525
5.4			342.06	4.475	347.56	4.478	347.11	4.482
5.3			311.57	4.440	316.42	4.446	315.86	4.448
5.2					285.29	4.423	284.73	4.423
5.1	243.54	4.405	250.61	4.398	253.90	4.407	253.40	4.406
5.0	213.05	4.392	219.49	4.389	221.91	4.398	221.56	4.395
4.9	181.87	4.386	187.40	4.388	188.95	4.395	188.83	4.392
4.8	149.61	4.385	153.79	4.393	154.57	4.399	154.71	4.396
4.7	115.76	4.390	117.87	4.405	118.11	4.407	118.45	4.405
4.6	79.66	4.397	78.61	4.416	78.63	4.417	78.91	4.417
4.5	42.77	4.368	39.93	4.364	39.93	4.364	39.94	4.364

difference. Comparison of the oceanic and continental dispersion curves of the preceding section indicates the approximate magnitude of the effect of path difference. The influence of phase shifts at continent-ocean boundaries is unknown but is minimized by restricting attention to successive great-circle traverses of a single phase. No attempt was made to correct the New Guinea–Pasadena path to a completely oceanic path. This correction is less than the 0.5 per cent accuracy estimated for these data.

Most of the group velocity points were determined directly from the records. Some of the New Guinea–Pasadena group velocity data were determined by numerical differentiation of the experimental phase velocity curve. Although the dispersion characteristics of inhomogeneous structures are completely specified by a phase velocity curve, group velocity data, although less accurate, are valuable corroborative information. The group velocity is a function of the actual values and the slope of the phase velocity curve and is, therefore, potentially useful for detecting subtle changes in the shape of the dispersion curve that may be overlooked owing to scatter if phase velocity data alone are considered. In the following analysis the group velocity is used as a loose extra constraint.

The CIT 6 oceanic model was used as a starting trial structure. To satisfy the New Guinea data we increased the velocity to 4.5 km/sec in the bottom half of the low-velocity zone. The resulting structure, CIT 8, gave a good fit to the data for periods less than 180 seconds. To satisfy the long-period data a discontinuity was introduced at 360 km. This structure, called CIT 9, was fairly satisfactory but fell above most of the free-oscillation data. A satisfactory fit was obtained by reducing the velocity in the depth interval 500 to 700 km. This resulted in a major discontinuity at 700 km. CIT 10 and 11, the final structures, give almost identical dispersion. CIT 11, a smoother structure, is here adopted as an oceanic model consistent with Love wave dispersion data. The parameters for the intermediate models, CIT 8, 9, and 10, are not of sufficient interest to reproduce in tabular form.

Figure 14 shows the shear velocity distribution for these models and, for comparison, the 8099 model of *Dorman et al.* [1960] and the Jeffreys-Bullen model. The 8099 structure was designed on the basis of Rayleigh wave data and flat-earth calculations. *Sykes et al.* [1962], on the basis of spherical calculations, consider it to be a satisfactory fit to oceanic data. *Kuo et al.* [1962], on the basis of an empirical correction to the flat-earth calculations, showed that data for Pacific Ocean paths fell slightly below the theoretical 8099 curve. They suggested

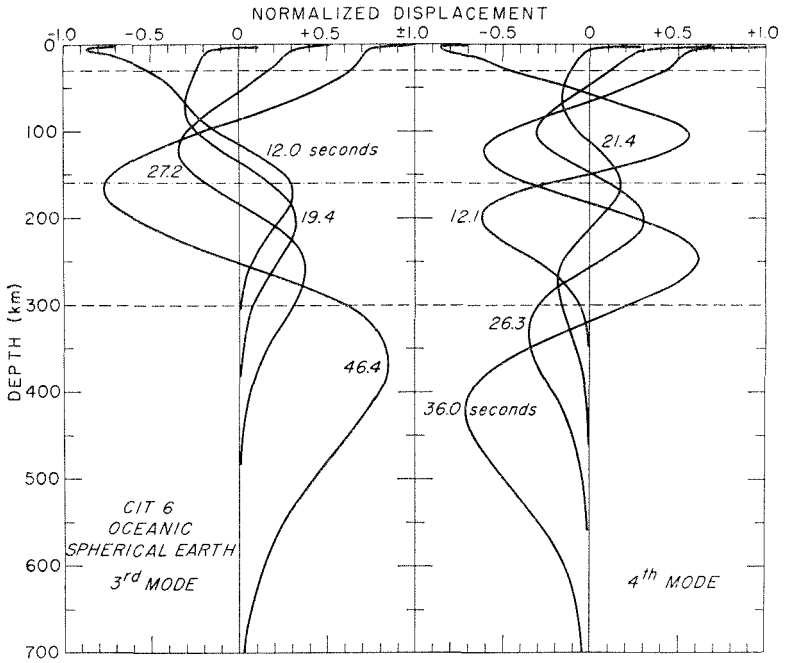

Fig. 12. Displacements for the third and fourth Love mode, CIT 6 structure.

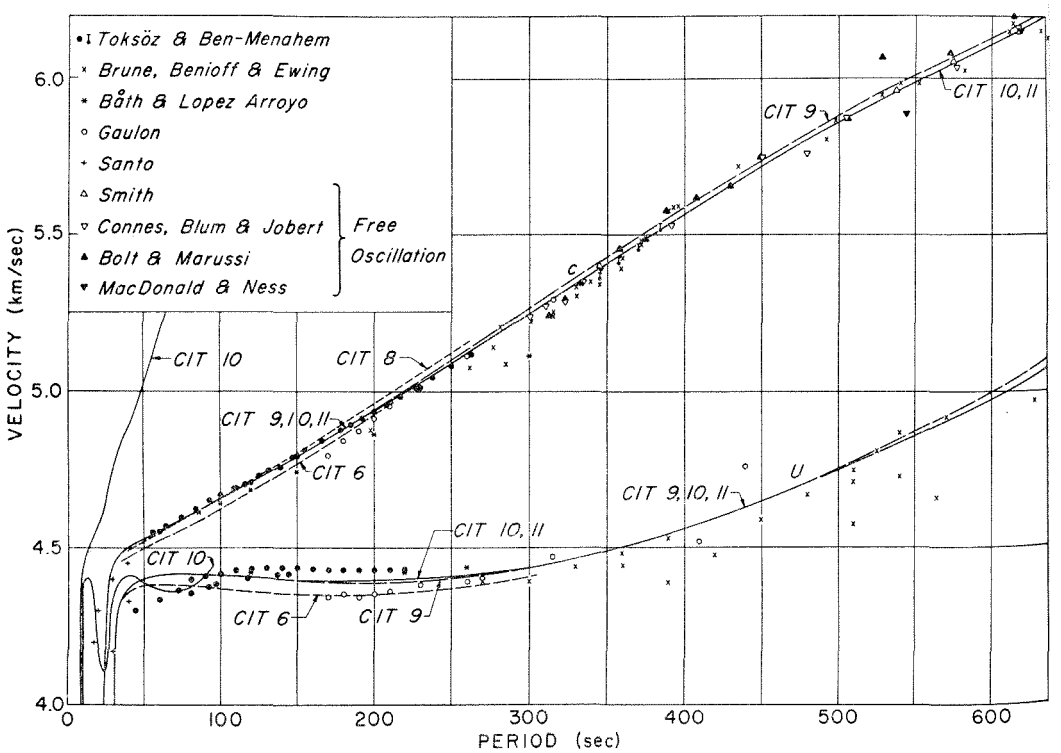

Fig. 13. Phase and group velocities for oceanic models CIT 6, 8, 9, 10, and 11 compared with Love wave dispersion and free torsional oscillation data. First higher mode is also shown for CIT 10.

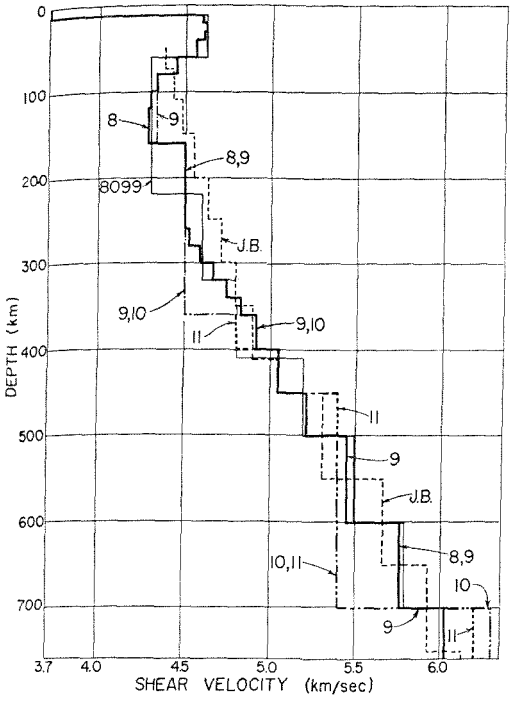

Fig. 14. Distributions of shear wave velocity for the oceanic models considered. Models 8099 and Jeffreys-Bullen (J. B.) are shown for comparison. CIT 11 is adopted as the structure consistent with the data for oceanic Love wave dispersion. Each model in the sequence 9 through 11 is identical with the preceding model except as otherwise indicated. See tables for details of the models.

that a slight decrease in the density or the shear velocity of the upper mantle was indicated.

The details of the upper crust are relatively unimportant for the periods considered here. Shorter periods are affected by the artificial surface layer in the oceanic model. This layer becomes a liquid layer in the Rayleigh wave calculations, which will be presented in a forthcoming paper. A conventional oceanic crust results in phase velocities slightly higher than those presented here at the shorter periods. For example, the fundamental mode for a typical oceanic crustal model is 0.01 km/sec higher at 70 seconds and the second mode is 0.025 km/sec higher at 10 seconds. The longer periods and higher modes are affected even less. Complete results for the crustal waveguide problem will be presented in a future paper.

Acknowledgment. This research was supported by grant AF-AFOSR-25-63 of the Air Force Office of Scientific Research as part of the Advanced Research Projects Agency project Vela.

References

Alterman, Z., H. Jarosch, and C. L. Pekeris, Propagation of Rayleigh waves in the earth, *Geophys. J., 4,* 219–241, 1961.

Anderson, Don L., Love wave dispersion in heterogeneous anisotropic media, *Geophysics, 27,* 445–454, 1962.

Anderson, D., Universal dispersion curves (unpublished manuscript), 1963.

Båth, M., and A. Lopez Arroyo, Attenuation and dispersion of *G* waves, *J. Geophys. Res., 67,* 1933–1942, 1962.

Bolt, B., and J. Dorman, Phase and group velocities of Rayleigh waves in a spherical, gravitating earth, *J. Geophys. Res., 66,* 2965–2981, 1961.

Bolt, B., and A. Marussi, Eigenvibrations of the earth observed at Trieste, *Geophys. J., 6,* 299–311, 1962.

Brune, J., H. Benioff, and M. Ewing, Long-period surface waves from the Chilean earthquake of May 22, 1960, recorded on linear strain seismographs, *J. Geophys. Res., 66,* 2895–2910, 1961.

Caloi, P., L'astenosfera Come Canale-guida dell'energia Sismica, *Ann. Geofis., 7,* 491–501, 1954.

Carr, R., and R. L. Kovach, Toroidal oscillations of the moon, *Icarus, 1,* 75–76, 1962.

Connes, J., P. A. Blum, G. and N. Jobert, Observation des oscillations propres de la terre, *Ann. Geophys., 18,* 260–268, 1962.

Dorman, J., M. Ewing, and J. Oliver, Study of shear velocity distribution by mantle Rayleigh waves, *Bull. Seismol. Soc. Am., 50,* 87–115, 1960.

Gaulon, R., Vitesse de groupe et vitesse de phase des andes de Love entre 160 et 315 seconds de periode, *Ann. Geophys., 18,* 298–299, 1962.

Harkrider, D., and D. L. Anderson, Energy and group velocity of surface waves (unpublished manuscript), 1963.

Haskell, N. A., Dispersion of surface waves on multi-layered media, *Bull. Seismol. Soc. Am., 43,* 17–34, 1953.

Jeans, J. H., The propagation of earthquake waves, *Proc. Roy. Soc. London, A, 102,* 554–574, 1923.

Kovach, R. L., and D. L. Anderson, Long-period Love waves in a heterogeneous spherical earth, *J. Geophys. Res., 67,* 5243–5255, 1962.

Kuo, J., J. Brune, and M. Major, Rayleigh wave dispersion in the Pacific Ocean for the period range 20-140 seconds, *Bull. Seismol. Soc. Am., 52,* 333–357, 1962.

MacDonald, G. J. F., and N. F. Ness, A study of the free oscillations of the earth, *J. Geophys. Res., 66,* 1865–1912, 1961.

Oliver, J., and M. Ewing, Normal modes of continental surface waves, *Bull. Seismol. Soc. Am., 48,* 33–49, 1958.

Santo, T. A., Dispersion of Love waves along various paths to Japan, 1, *Bull. Earthquake Res. Inst., Tokyo Univ., 40,* 631–652, 1962.

Smith, S., An investigation of the earth's free oscillations, Thesis, California Institute of Technology, Pasadena, 1961.

Sykes, L., M. Landisman, and Y. Satô, Mantle shear velocities determined from oceanic Love and Rayleigh wave dispersion, *J. Geophys. Res., 67,* 5257–5271, 1962.

Toksöz, M. N., and A. Ben-Menahem, Velocities of mantle Love and Rayleigh waves over multiple paths, *Bull. Seismol. Soc. Am., 53,* in press, 1963.

Yanovskaya, T. B., The dispersion of Rayleigh waves in a spherical layer, *Bull. Acad. Sci. USSR, Geophys. Ser. No. 7,* 801–817, 1958.

(Manuscript received February 11, 1963; revised March 28, 1963.)